

## Bond nature of oxygen-deficient HfO<sub>2</sub>/Si(100) film

Deok-Yong Cho, C.-H. Min, Jungho Kim, and S.-J. Oh<sup>a)</sup>

CSCMR, School of Physics and Astronomy, Seoul National University, Seoul 151-747, Korea

Min Gyu Kim

Pohang Accelerator Laboratory, POSTECH, Pohang 790-784, Korea

(Received 21 June 2006; accepted 12 November 2006; published online 21 December 2006)

The authors investigate the bonding environment of an oxygen-deficient HfO<sub>2</sub>/Si film grown by means of pulsed laser deposition, by analyzing the Hf *L*<sub>3</sub>-edge extended x-ray absorption fine structure. The local characteristics around the Hf atom, such as the bond length or the number of nearest neighbors, are found to depend on the oxygen supply during film growth. The chemical states of these samples are also probed *in situ* by x-ray/ultraviolet photoelectron spectroscopies. The core-level binding energy and the work function for each sample are found to be correlated with the mean Hf–O bond length, implying a close connection between the chemical environment and bond nature. © 2006 American Institute of Physics. [DOI: 10.1063/1.2410214]

Hafnia (HfO<sub>2</sub>) is promising as the complementary gate oxide material in nanoscale memory devices. However, before it can be used extensively, one of the difficulties that needs to be overcome is the defect problem. When HfO<sub>2</sub> has point defects such as atomic vacancies or interstitial atoms, the electrical characteristics get severely degraded because the defect site traps hole or electron carriers and induces a leakage current. With regard to the electronic structure, the defects are described to form extrinsic defect energy levels in the bulk band gap of HfO<sub>2</sub>, such that the position of the Fermi level ( $E_F$ ) or work function of the system changes. Hence, it is quite important to investigate the possible point defects and their characteristics in HfO<sub>2</sub>.<sup>1–3</sup>

Some of the present authors have recently discussed the role of oxygen vacancies in HfO<sub>2</sub> on the characteristics of the oxide and the interfaces.<sup>4</sup> Theoretically, the oxygen vacancy levels are expected to be above the genuine  $E_F$ ;<sup>5–7</sup> therefore, the effective  $E_F$  increases in the presence of oxygen vacancies. Further, when a vacancy is formed, it should concurrently involve a relaxation process in order to reduce the total energy of the system: a change in the Hf–O bond length is primarily expected.<sup>8</sup> Also, this relaxation process naturally involves a redistribution of charges, since the Hf and O atoms are bound with an ionic Madelung interaction; this initiates a change in their chemical states. Thus the close relation between the chemistry of the Hf–O bond and the local physical properties such as bond length and the number of nearest neighbors is expected. However, no experiment has been performed in order to investigate this interconnection. In this letter, we present an experimental study on this subject by using extended x-ray absorption fine structure (EXAFS) technique to investigate the local geometry around the oxygen defect and simultaneously by using x-ray/ultraviolet photoelectron spectroscopy (XPS/UPS) measurements to investigate the chemical states. HfO<sub>2</sub> films with different oxygen contents can be easily grown by controlling the external supply of oxygen during the film growth;<sup>9</sup> these films are expected to exhibit differences in both the chemical ( $E_F$ ) (Ref. 10) and physical (bond length) properties. Indeed,

in these films, we found that the  $E_F$  and the Hf–O bond length are strongly correlated.

The HfO<sub>2</sub> films (~20 Å) were deposited onto a HF-etched *p*-Si(100) substrate with a 3 Hz pulsed neodymium-doped yttrium aluminum garnet laser at a substrate temperature of 700 °C. Each sample was grown under distinct growth conditions. One of the samples was deposited under an additional oxygen supply ( $P_0=1 \times 10^{-4}$  Torr) to eliminate Hf silicide<sup>9</sup> and then annealed for 5 min at 700 °C in vacuum to improve the film stoichiometry (sample 1). Another sample was grown with no oxygen supply and annealed in vacuum for 5 min (sample 2). The third sample was also grown with no oxygen supply but was not annealed (sample 3). Measurements using XPS and UPS were then performed *in situ* to detect both the core-level binding energy (BE) shifts and the onsets of secondary electrons (SEs) in these samples. The oxygen concentration in HfO<sub>*x*</sub> could be deduced from the area ratio of O 1*s*/Hf 4*f* peaks in the XPS spectra, and the value for sample 3 was about  $x=1.8–1.9$  (i.e., 5%–10% oxygen deficiency). Subsequently, the Hf *L*<sub>3</sub>-edge ( $h\nu \sim 9.56$  keV) x-ray absorptions were measured in the fluorescence yield mode at the 7C beamline in Pohang Light Source (PLS). To obtain the surface sensitive information of ultrathin HfO<sub>2</sub> films and their interfaces, the incident beams were glanced off the sample planes by 2°.

A hard x-ray absorption measures the transition on a specific atom from a deep core level to elastically scattered wave functions. By Fourier transforming (FT) the background-subtracted absorption coefficients [ $\chi(E)$ ], the local atomic distribution can be determined by analyzing the EXAFS.<sup>11</sup> Our EXAFS data were processed using a standard UWXAFS 3.0 package onto  $k^2$ -weighted  $\chi(k)$  with a  $k$ -cut range of 2–8 Å<sup>-1</sup>. The FT spectra (indicated by markers) versus  $R$  are shown in Fig. 1, where  $R$  denotes the radial distance from the photon-absorbing atom to the scatterer atom without considering the phase shift of the final-state wave function during the scattering process. The raw absorption spectra versus photon energy are also shown in the inset. For comparison, the EXAFS of a HfO<sub>2</sub> powder (monoclinic, 5 mm thick) is also shown at the bottom ( $k$ -cut range of 2–12 Å<sup>-1</sup>). The large peaks at  $R < 2.0$  Å (first shell) repre-

<sup>a)</sup>Electronic mail: sjoh@plaza.snu.ac.kr

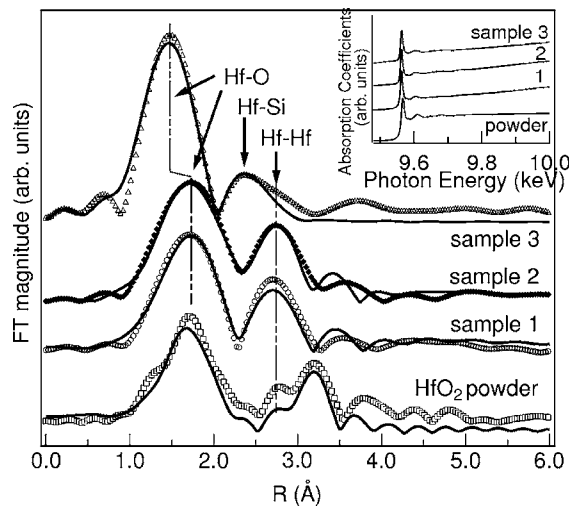


FIG. 1. EXAFS spectra ( $FT[k^2\chi(k)]$ , markers) in the  $R$  space, probing the neighboring atoms of Hf (O, Si, and Hf) with their fitting lines (solid lines) and appropriate peak attributions. The difference in the mean Hf–O bond lengths is evident between samples 1 and 2 ( $\sim 2.16$  Å) and sample 3 ( $\sim 2.03$  Å). The relevant fitting parameters are listed in Table I. The  $k$ -cut range is  $2\text{--}8$  Å $^{-1}$  except that for HfO<sub>2</sub> powder ( $2\text{--}12$  Å $^{-1}$ ).

sent the Hf–O bonds and those in  $2.0$  Å  $< R < 3.5$  Å (second shell) are mainly (indirect) Hf–Si/Hf bonds.

Fitting was performed in the  $R$  space, based on a single backscattering model up to the second shell.<sup>12</sup> Following the fitting results, we can determine the local information near a specific atom, such as the scattering amplitudes or the amount of phase correction ( $\Delta$ ); the fitting parameters are summarized in Table I. The *mean* interatomic distances obtained from the fitting are listed in Table I; they are indicated as the  $R+\Delta$  values. It is noteworthy that the mean Hf–O distance of sample 3 (2.03 Å) is less than those of sample 1 (2.17 Å) and sample 2 (2.16 Å). This shorter bond length can be attributed to the relaxation due to vacancy formation. Since the Hf–O bond is ionic with opposite charges on either side, the Hf and O atoms tend to attract each other. Therefore, the Hf atom is in its equilibrium position for attractive interactions with the surrounding oxygen atoms. However, when one of the surrounding oxygen atoms is eliminated, the equilibrium is broken and the nearest Hf atoms migrate outwards from the vacancy site; therefore, these atoms are in another equilibrium position closer to the other oxygen atoms than they were before. This argument is in agreement with the result of a density functional theoretical study that includes the lattice relaxation effects.<sup>8</sup> Thus, if the oxygen vacancy influences the bond-length change, the number of

TABLE I. First shell EXAFS fitting parameters where  $N$  is the number of the nearest neighboring atomic species,  $R+\Delta$  is the phase-corrected real atomic distances, and  $\sigma^2$  is the disorder (Debye-Waller) factor, along with the relative Fermi level with respect to that of sample 1. In the EXAFS fitting, a reduction factor  $S_0^2$  due to the breakdown of the frozen-orbital approximation is set to unity in this table.

	EXAFS (Fig. 1)			XPS/UPS
	$N(\text{Hf-O})$	$R+\Delta(\text{Hf-O})$ (Å)	$\sigma^2$ (Å <sup>2</sup> )	(Figs. 2 and 3) $E_F$
Sample 1	$7.0 \pm 1.4$	$2.165 \pm 0.019$	$0.013 \pm 0.004$	...
Sample 2	$6.8 \pm 1.4$	$2.157 \pm 0.019$	$0.013 \pm 0.004$	+0.05
Sample 3	$6.2 \pm 1.3$	$2.029 \pm 0.020$	$0.006 \pm 0.005$	+0.3

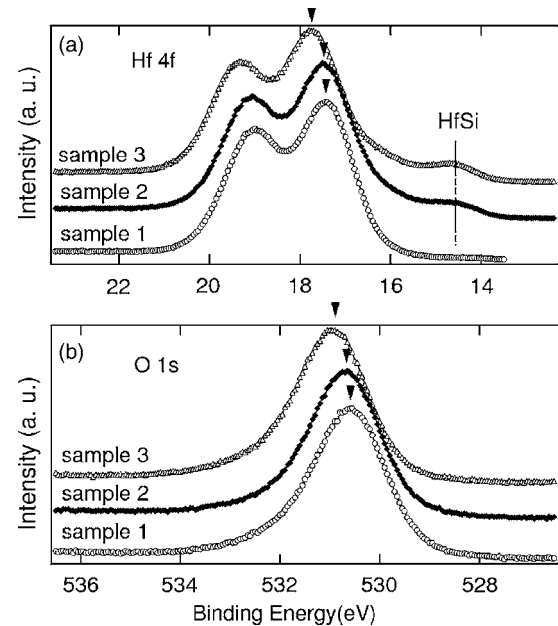


FIG. 2. XPS spectra of Hf 4*f* (a) and O 1*s* (b) core levels for the three samples. The BE shifts measured by the positions indicated by black triangles are listed in Table I.

oxygen atoms surrounding the Hf atom should also decrease. A relative decrease in the number of nearest neighbors ( $\#nn$ ) is evident in sample 3 when compared with those of samples 1 and 2; this can be observed in Table I. Therefore we can confirm that the oxygen defects reduce the mean Hf–O distance as well as  $\#nn$ .

Further,  $\#nn$  and the Hf–O length of sample 2 are quite similar to those of sample 1. This implies that annealing “cures” the oxide filling up the vacancies. Although the manner in which annealing assists oxidation has not been well clarified, we can qualitatively assume that the vacancy formation costs energy:<sup>8</sup> a transition from the relaxed-vacant state to the stoichiometric state corresponds to that from the local minimum to the grand minimum of total energy of the system; therefore, heat (annealing) is required to overcome the threshold energy.

In the second shell, we observe an increase in the intensity in the lower- $R$  side ( $R \sim 2.3$  Å) in the spectrum of sample 3, while the maxima of the second shells in the spectra of samples 1 and 2 are observed at  $R \sim 2.7$  Å. The second shell in the spectra of samples 1 or 2 can be interpreted as a Hf–Hf bond. However, the second shell of sample 3 cannot be interpreted as the Hf–Hf bond shortened by  $-0.4$  Å; this is because the atomic distances in a crystal are primarily determined by the atomic sizes, which cannot vary as much as  $0.4$  Å. Instead, it probably represents a typical Hf–Si bond. This interpretation is corroborated by the fact that the number of metallic Hf–Si bonds in sample 3 is greater than those in the other samples, as will be shown in the core-level XPS data [Fig. 2(a) below].

We also performed XPS and UPS measurements on the same samples to determine the chemical state of each atom. Since the XPS/UPS spectra were measured just after the sample deposition while maintaining the vacuum, the measurements were free from surface contaminations. In Fig. 2, (a) Hf 4*f* and (b) O 1*s* XPS spectra of the three samples are shown. The Hf 4*f*<sub>7/2</sub> main peaks ( $\sim 17.4$  eV) in Fig. 2(a) are attributed to the Hf<sup>4+</sup> in HfO<sub>2</sub>,<sup>13</sup> and the small features in the

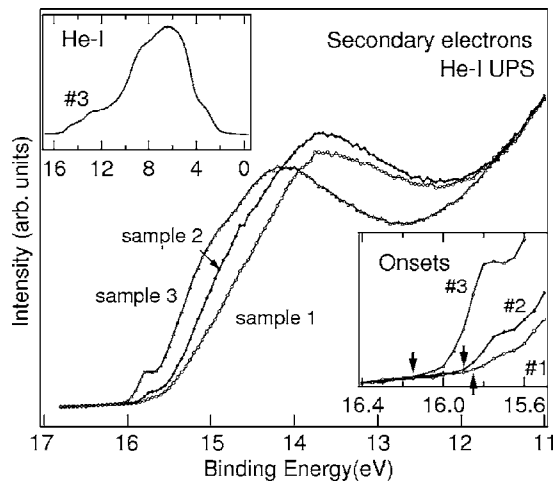


FIG. 3. Onsets of the secondary electrons in He I ( $h\nu=21.2$  eV) UPS spectra. For clarity, a typical wide scan from sample 3 is appended in the upper inset. The high BE region is magnified in the figure, and the lower inset shows further magnification. The BE positions determined as the onsets of SEs are denoted by arrows.

lower BE side should be attributed to Hf silicide ( $\text{Hf}_x\text{Si}_y$ ) as described earlier.<sup>9</sup> Note that this small feature does not exhibit a shift in the BE as opposed to the main peak; this can be observed in the comparison of the spectra of samples 2 and 3. This clearly indicates that the shift in the main peak does not originate from experimental artifacts such as sample charging. The same amount of BE shifts with the Hf  $4f$  main peaks are observed in the O  $1s$  peaks in Fig. 2(b). The line shapes of the peaks are also similar with each other, indicating that the O–Hf bonds ( $\text{BE} \sim 530.6$  eV) are dominant and the number of O–Si bonds ( $\text{BE} \sim 532.7$  eV) is insignificant. Thus, the formation of Si oxide has negligible effect in these systems. If the measured BE shifts were related to an experimental chemical shift attributed to a change in the Madelung potential or that in the number of valence charges, the BE shifts measured in the Hf  $4f$  and O  $1s$  spectra should have opposite signs since a charge transfer occurs between the Hf and O atoms. The fact that the shifts are in the same direction indicates that the BE shifts represent a change in  $E_F$  in the  $\text{HfO}_2$  film. This argument is corroborated by the fact that the amount of BE shift coincides with that of the onset of SEs in the UPS spectra, as will be shown in Fig. 3.

The UPS spectra were obtained using the He I source ( $h\nu=21.2$  eV), and a typical wide scan (of sample 3) is shown in the upper inset. The features at  $\text{BE}=4\text{--}10$  eV are commonly known to originate mainly from the O  $2p$  of  $\text{HfO}_2$ ,<sup>7,14</sup> and the bump in the right-hand side shoulders in  $\text{BE}=2\text{--}4$  eV could be partially attributed to the “metallic” Hf–Si valence bands since they develop with the Hf–Si peak in Fig. 2(a). The feature in the higher BE side ( $\text{BE} > 12$  eV) comprises mainly SEs, i.e., photoelectrons that have lost their kinetic energies during the intrinsic or extrinsic energy loss process in the solid. In general, these SEs have a continuous kinetic energy distribution with zero lower bound. Thus, any change in the onset of the SEs indicates the  $E_F$  change. We magnified this region in Fig. 3; further magnification was carried out near the onset, as seen in the lower inset. The BE positions determined as the onsets of SEs are

denoted by arrows. The difference of SE onsets between the spectra of sample 3 and those of samples 1 and 2 is clearly observed. The amount of  $E_F$  shift for each sample, as observed in Fig. 3, coincides with the value deduced from Figs. 2(a) and 2(b). The relative shifts in Figs. 2 and 3 with respect to sample 1 are listed in Table I.

The distinct feature of sample 3 from samples 1 and 2 is observed at both the Hf  $L_3$ -edge EXAFS and the XPS/UPS measurements. This indicates that the local Hf–O bond environments are strongly correlated with the chemical characteristics of the  $\text{HfO}_2$  films. In the absence of additional oxygen supply during the film growth or postannealing as in sample 3, oxygen defects are easily formed in  $\text{HfO}_{x<2}/\text{Si}$ ; this increases the  $E_F$  of the  $\text{HfO}_{x<2}$  film and reduces the Hf–O bond length.<sup>5</sup> After annealing as in sample 2, however, both the  $E_F$  and the Hf–O bond length are almost recovered. Therefore, the correlation between  $E_F$  and the Hf–O bond length is confirmed.

In conclusion, we have investigated the effects of oxygen vacancy on the Hf–O bonding environments and their chemical states by using EXAFS and XPS/UPS measurements. It is shown that the mean Hf–O bond length and the number of nearest neighbors clearly depend on the oxygen supply during film fabrication and postannealing. The chemical states of  $\text{HfO}_{x<2}$  are also found to depend on the oxygen supply and postannealing. Finally, a close relationship between the chemical states of the  $\text{HfO}_{x<2}$  and the mean Hf–O bond length is confirmed.

This study is supported by the Korean Science and Engineering Foundation through the Center for Strongly Correlated Materials Research at the Seoul National University, and the experiments at PLS were supported in part by MOST and POSTECH.

- <sup>1</sup>K. Xiong, J. Robertson, and S. J. Clark, *Phys. Status Solidi B* **243**, 2071 (2006).
- <sup>2</sup>H. Takeuchi, D. Ha, and T.-J. King, *J. Vac. Sci. Technol. A* **22**, 1337 (2004).
- <sup>3</sup>N. V. Nguyen, A. V. Davydov, D. Chandler-Horowitz, and M. M. Frank, *Appl. Phys. Lett.* **87**, 192903 (2005).
- <sup>4</sup>D.-Y. Cho, S.-J. Oh, Y. J. Chang, T. W. Noh, R. Jung, and J. C. Lee, *Appl. Phys. Lett.* **88**, 193502 (2006).
- <sup>5</sup>J. Robertson, K. Xiong, and S. J. Clark, *Thin Solid Films* **496**, 1 (2006).
- <sup>6</sup>K. Xiong, J. Robertson, M. C. Gibson, and S. J. Clark, *Appl. Phys. Lett.* **87**, 183505 (2005).
- <sup>7</sup>P. W. Peacock and J. Robertson, *Phys. Rev. Lett.* **92**, 057601 (2004).
- <sup>8</sup>A. S. Foster, F. L. Gejo, A. L. Shluger, and R. M. Nieminen, *Phys. Rev. B* **65**, 174117 (2002).
- <sup>9</sup>D.-Y. Cho, K.-S. Park, B.-H. Choi, S.-J. Oh, Y. J. Chang, D. H. Kim, T. W. Noh, R. Jung, and J. C. Lee, *Appl. Phys. Lett.* **86**, 041913 (2005).
- <sup>10</sup>D. Lim, R. Haight, M. Copel, and E. Cartier, *Appl. Phys. Lett.* **87**, 072902 (2005).
- <sup>11</sup>R. Puthenkavilakam, Y.-S. Lin, J. Choi, J. Lu, H.-O. Blom, P. Pianetta, D. Devine, M. Sendler, and J. P. Chang, *J. Appl. Phys.* **97**, 023704 (2005).
- <sup>12</sup>This is enough to get the physical properties of the first two shells, despite the lack of fit between the modeled and experimental EXAFS data at high- $R$  ( $>3.5$  Å) regions.
- <sup>13</sup>Unlike the EXAFS data in Fig. 1, the contribution of Hf–Hf bond is not evident here in XPS. This is because XPS shows information on the chemistry of Hf ion, which is mostly determined by the Hf–O hybridization strength only.
- <sup>14</sup>S. Sayan, T. Emge, E. Garfunkel, Xinyuan Zhao, L. Wielunski, R. A. Bartyński, David Vanderbilt, J. S. Svehle, S. Suzer, and M. Banaszak-Holl, *J. Appl. Phys.* **96**, 7485 (2004).